Identification of Microphases in Mixed α- and ω-Gliadin Protein Films Investigated by Atomic Force Microscopy

Terence J. McMaster,*,† Mervyn J. Miles,† Lars Wannerberger,‡ Ann-Charlotte Eliasson,‡ Peter R. Shewry,§ and Arthur S. Tatham§

H. H. Wills Physics Laboratory, University of Bristol, Tyndall Avenue, Bristol BS8 1TL, United Kingdom, Department of Food Technology, Lund University, P.O. Box 124, Getingevagen, Lund S-221 00, Sweden, and IACR−Long Ashton Research Station, Department of Agricultural Sciences, University of Bristol, Long Ashton, Bristol BS41 9AF, United Kingdom

Pure and mixed films of α- and ω-gliadins were studied by tapping mode atomic force microscopy (AFM). The technique was sensitive to the chemistry of the surface properties of the films, allowing imaging of the mixed gliadin phases at different ratios. In addition to the study of the phases at the micrometer level, higher resolution images allowed visualization of the protein films at the molecular level. These studies may have relevance to the formation of phases in developing protein bodies in grain, where gliadins and glutenins are deposited together. It has been assumed that the protein bodies consist of a random network of proteins; these studies indicate that microphases could be present in protein bodies. The technique provides novel methods for studying mixed biopolymer systems.

Keywords: *Gliadin; atomic force microscopy; AFM; phase angle; protein film*

INTRODUCTION

The alcohol-soluble seed storage proteins, prolamins, of cereal seeds consist of a complex heterogeneous mixtures of components (Shewry and Tatham, 1990). In wheat they are classified into two groups on the basis of their aggregative properties. The gliadins are monomeric proteins and are divided into four groups, the α-, β-, γ-, and ω-gliadins, on the basis of their electrophoretic mobilities at low pH (Woychik et al., 1961). The α-, β-, and γ-gliadins are structurally related, consisting of repetitive N-terminal and nonrepetitive C-terminal domains, with three or four intramolecular disulfide bonds (Shewry and Tatham, 1997). The ω-gliadins are structurally distinct, consisting of a single repetitive domain with no cysteine residues and consequently no disulfide bonds (Tatham and Shewry, 1995). The gliadins interact by hydrogen bonding and hydrophobic interactions and contribute to the viscous nature of gluten. In contrast, the glutenins form disulfide-bonded polymers, made up of high and low M_r subunits and contribute to gluten elasticity. Together the gliadins and glutenins are responsible for the unique viscoelastic properties of wheat glutens and doughs.

In α-gliadins the two domains are of approximately equal length, with the repetitive N-terminal domain consisting of two repeat motifs (consensus Pro.Gln.Gln.Pro.Tyr and Pro.Gln.Pro.Gln.Pro.Phe.Pro) and the nonrepetitive C-terminal domain containing most of the charged amino acid residues and three disulfide bonds. Structural studies indicate that the proteins adopt a

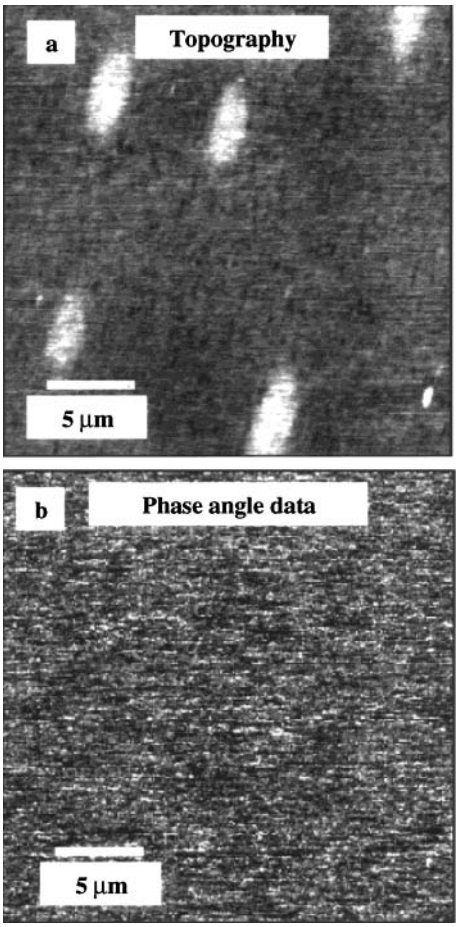

Figure 1. Tapping mode topograph and phase angle data for a single-component α-gliadin film.

* Author to whom correspondence should be addressed [telephone +44 (0)117 9289000, ext. 8744; fax +44 (0)117 9255624; e-mail t.mcmaster@bristol.ac.uk].

† H. H. Wills Physics Laboratory, University of Bristol.

‡ Lund University.

§ IACR−Long Ashton Research Station, University of Bristol.

10.1021/jf9904057 CCC: $18.00
Published on Web 11/20/1999

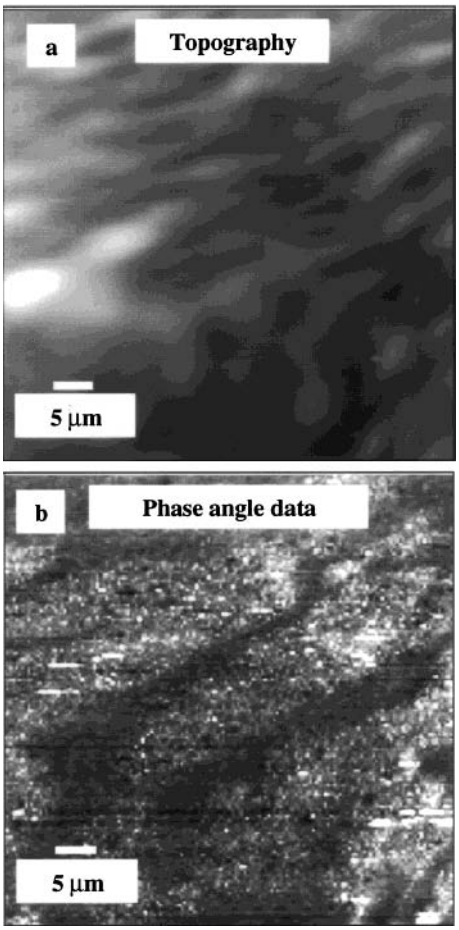

Figure 2. Tapping mode topograph and associated phase angle data of a 1:1 (w/w) mixed α- and ω-gliadin LB film. The images are 50 μm square, and the *z* scales on the images are 0−500 nm (topograph) and 0−60° (phase data). (Figure is reproduced here at 75% of the original.)

globular conformation (Cole et al., 1984; Shewry et al., 1997), the nonrepetitive domain being predominantly α-helical and the repetitive domain adopting a β-reverse turn-rich structure (Tatham and Shewry, 1985). The ω-gliadins consist predominantly of a single repeat motif (consensus Pro.Gln.Gln.Pro.Phe.Pro.Gln.Gln) and interact via hydrogen bonding through the glutamine residues. Their secondary structure consists of an equilibrium between β-reverse turns and poly-L-proline II-like structure (Tatham et al., 1989), and they appear to be rodlike in solution (Field et al., 1986; Shewry et al., 1997). Therefore, the α- and ω-gliadins are distinct in their sequences and conformations.

Atomic force microscopy (AFM) of proteins is providing high-resolution images of both individual molecules (Bergkvist et al., 1998; Hallet et al., 1996; Leggett et al., 1996; Marchant et al., 1997; van Noort et al., 1998; Schneider et al., 1998) and protein arrays and membranes (Furuno et al., 1998; Müller et al., 1997, 1998; Ohnishi et al., 1996; Wannerberger et al., 1997; McMaster et al., 1996; Rakowska et al., 1998). In addition, it allows the mapping of the "chemical" nature of a surface, which we have exploited to study films of mixtures of α- and ω-gliadins. This shows that they form separate phases, which may be relevant to how the different types of gluten proteins interact in the developing grain and in gluten and dough systems.

EXPERIMENTAL METHODS

Protein Purification. α- and ω-gliadins were prepared as described by Wannerberger et al. (1997) and Wellner et al. (1996), respectively. Purity was determined by SDS−PAGE and acid−PAGE.

AFM. AFM was carried out using tapping mode imaging in air using a Digital Instruments Multimode instrument (Digital Instruments, Santa Barbara, CA). In this mode, the cantilever is oscillated just below its resonant frequency and is brought into intermittent tapping contact with the sample. As it taps the sample, both the amplitude of the oscillation and the phase angle relative to that at the resonant peak are affected. The amplitude decreases because the tip strikes the surface, and this reduction in amplitude is measured. When controlled with feedback circuitry to tap at constant amplitude, this measurement can be used to construct a topographic map of the surface. Simultaneously the phase angle shift is monitored pixel by pixel to yield information on the material properties of the sample. Previous work using tapping mode has shown it to be sensitive to the elastic, viscoelastic, and adhesive properties of the sample material (Garcia et al., 1998, and references cited therein). In this study, silicon cantilevers of spring constant 30 Nm^{-1} and resonant frequency 300 kHz were used (manufacturer's approximate figures). Off-line image processing and image analysis were carried out using proprietary software packages (Digital Instruments).

Protein Films. The Langmuir−Blodgett (LB) films were prepared using the methods described previously in Wannerberger et al. (1997). For the adsorbed films, the α- and ω-gliadin proteins were readily dissolved to 0.1 mg L^{-1} in 70% aqueous ethanol (spectrophotometric grade, Sigma, U.K.). The mixed solutions were prepared in the ratios 1:3, 1:1, and 3:1 (v/v). A 1 cm^2 piece of mica was freshly cleaved to present an atomically flat, clean surface. A 5 μL aliquot of the appropriate protein solution was pipetted onto the surface and allowed to evaporate to dryness. The samples were examined between 2 and 12 h after deposition.

RESULTS AND DISCUSSION

Figure 1 consists of a pair of images collected simultaneously from the same area of an LB film prepared from α-gliadin. The constant tapping amplitude data, or topography, show a very flat surface punctuated by small ellipsoidal hillocks. The phase angle data show little or no contrast across the image area, indicating a uniformity of composition of the surface, consistent with the sample preparation. The localized higher regions would appear to be the result of the surface preparation technique, and it is interesting to note that they are all oriented in the same direction, perhaps as a result of compression. Figure 2 provides an interesting comparison with Figure 1. The surface topography of this mixed α- and ω-gliadin LB film shows a rippled texture, again as a result of the preparation conditions, but the accompanying cantilever phase angle image presents a surface with two different intensity levels (light and dark) irrespective of the changes in local topography. This indicates the presence of two components with differing surface properties which then influence the behavior of the oscillating cantilever as it taps the surface. Because the α- and ω-gliadins might be expected to have similar values for elastic modulus, it is likely that differences in surface adhesion would provide a contrast mechanism. The α-gliadin molecule possesses more charged residues than the ω-gliadin molecule and would therefore be more hydrophilic in character in the ambient air imaging environment. The tip surface is likely to be terminated in oxide or hydroxyl groups and is hydrophilic. Force interaction spectroscopy using AFM has shown that there is greater adhesion between

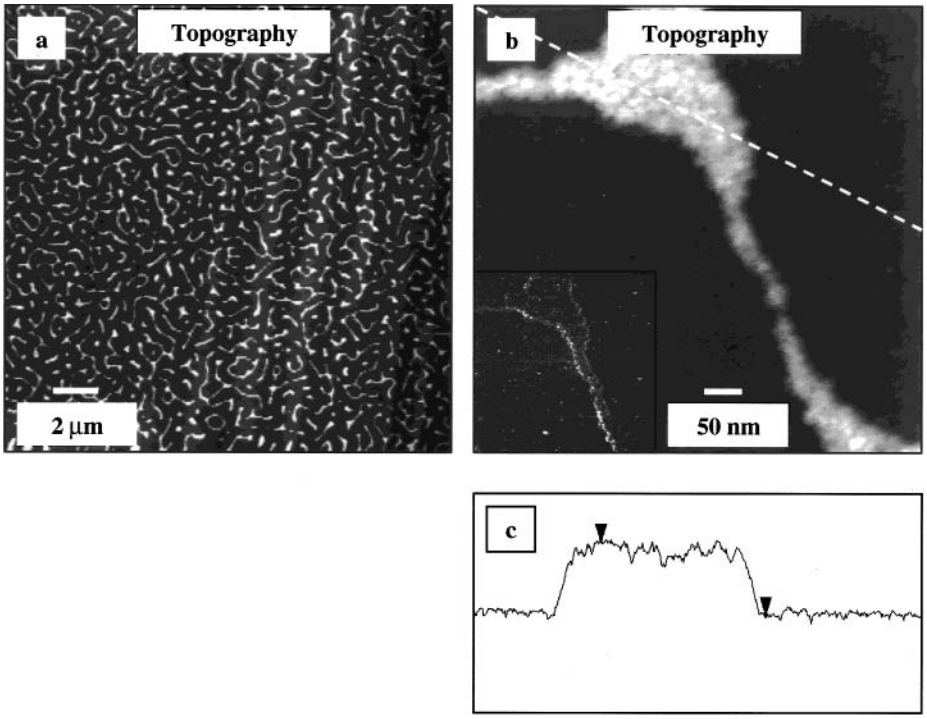

Figure 3. Single-component ω-gliadin film adsorbed from 5 μL of a 0.1 mg mL^{-1} solution in 70% aqueous ethanol: (a) constant tapping amplitude topographic data, 0−6 nm z scale; (b) high-resolution topograph and associated phase data (inset); (c) line profile along dashed line in (b). The height difference between the arrows is 2 nm.

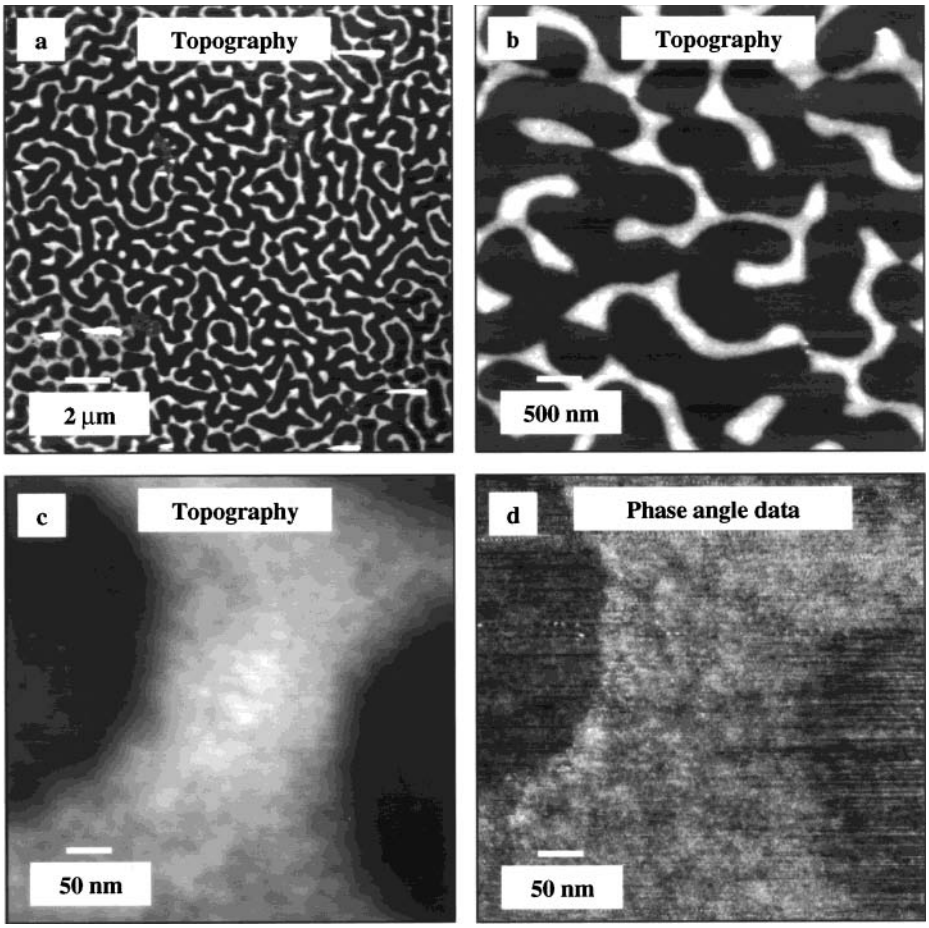

Figure 4. (a, b) Two topographic images of the surface of a 1:3 α/ω (w/w) mixed gliadin film evaporated from solution. The z scales are 0−10 nm in both images. (c, d) 500 nm high-magnification image and accompanying phase data showing a marked phase angle difference between the two regions of the surface. z scales are 0−10 nm and 0−20°, respectively.

like surfaces than between unlike surfaces (Frisbie et al., 1994), and this is probably the source of the phase angle contrast for the mixed LB film. An analysis of the relative surface area coverage of Figure 2b shows 59 ±

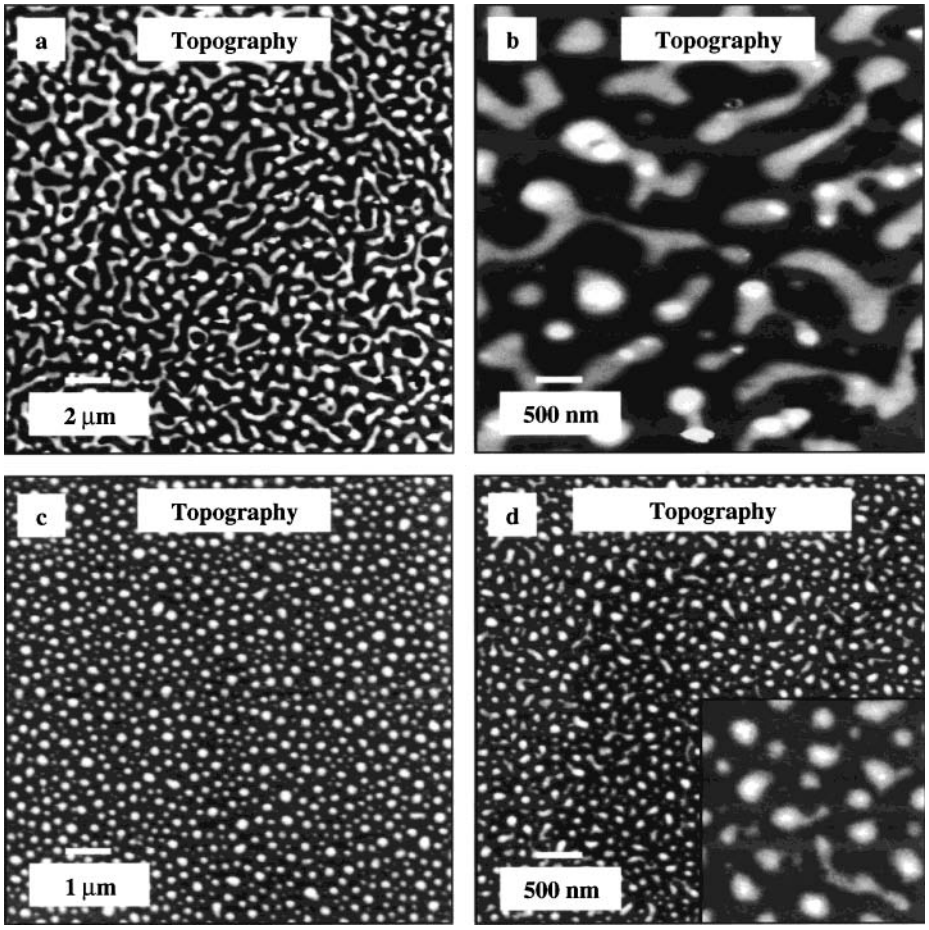

Figure 5. (a−d) Four topographic images of the surface patterns produced from a 1:1 α/ω (w/w) mixed film deposited from solution. The height scales are 0−15, 0−15, 0−10, and 0−7.5 nm, respectively. The inset in (d) is an 800 nm scan of the surface texture.

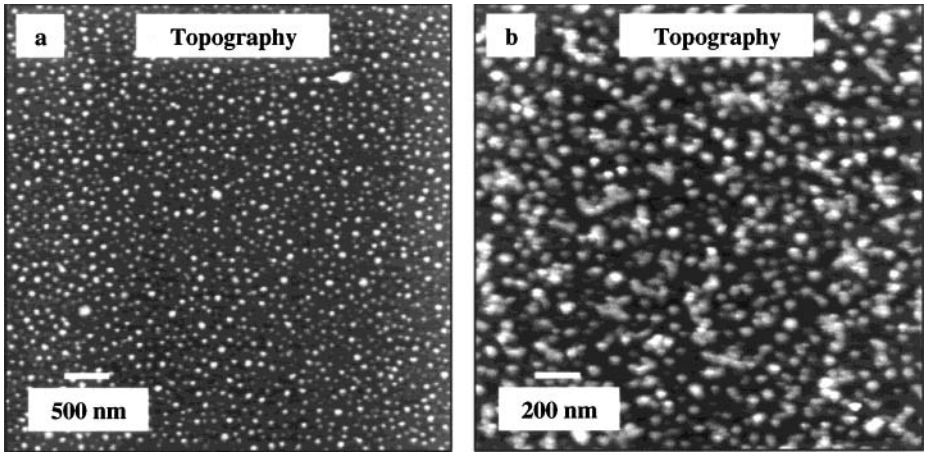

Figure 6. (a, b) Surface morphology of a 3:1 α/ω gliadin film. *z* scale is 0−5 nm in both images.

3% light and 41 ± 3% dark areas, in keeping with the composition of the mixed film (1:1). The light and dark domains in Figure 2b are aligned in a similar direction to the surface rippling in Figure 2a, which may indicate a surface pressure ordering effect for this system.

The morphology of a 100% ω-gliadin film obtained on adsorption from solution (Figure 3a) appears to show the presence of more than a single layer of protein. Structures are observed in a range of shapes such as loops, filaments, and toroids, but all are of a uniform height, 1−2 nm. Figure 3b shows one such feature in more detail. The height profile along the dashed white line of Figure 3b is shown in Figure 3c, and the height difference between the markers is 1.9 nm. The height variation is consistent with a ω-gliadin molecule in a horizontal alignment on the surface. The conformation of the structurally homologous barley protein, C hordein, is known from viscometric measurements to be rodlike with length of ∼30 nm and width of 2 nm in solution (Field et al., 1986). The lower area of the surface appears to be similar in texture to the raised portion, and this is confirmed by inspection of the phase angle data for the same area (see inset). There is also no phase angle difference between the two regions apart from a small increase in intensity at the edge of the raised area, suggesting that this artifact is caused by

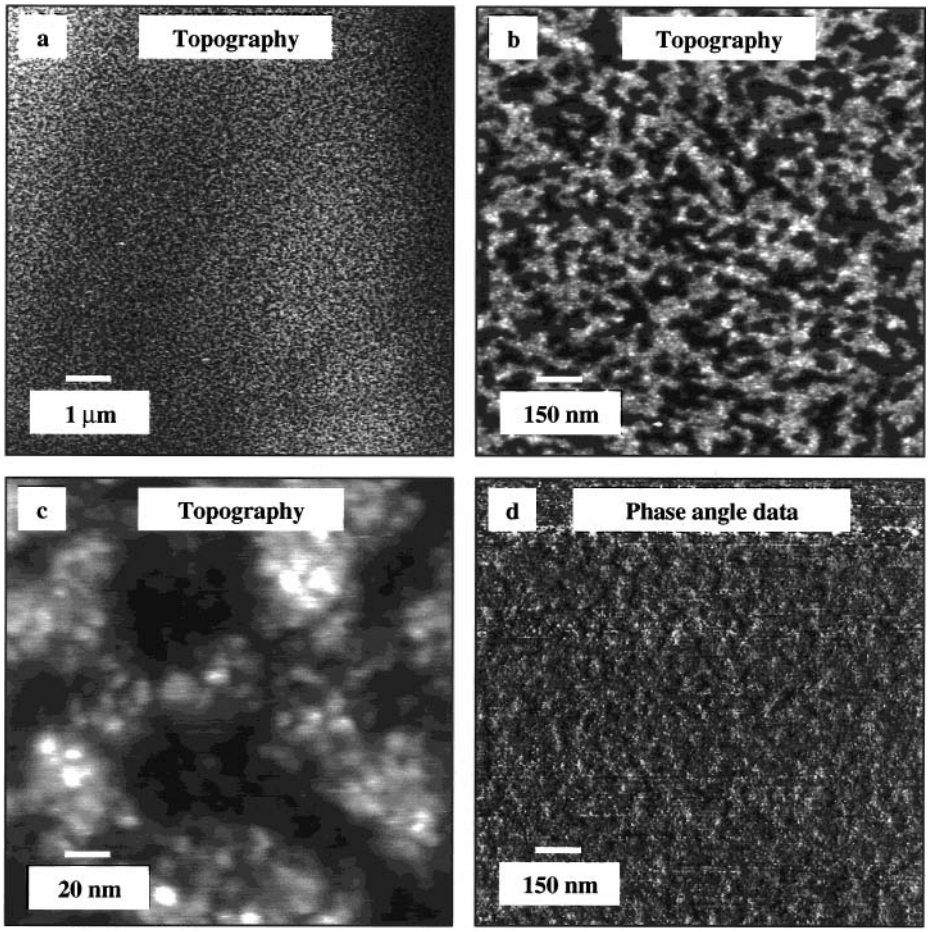

Figure 7. Single-component ω-gliadin film produced by evaporation: (a, b) 10 and 1.5 μm images with 0−5 nm z scale; (c) 200 nm topographic image, z scale of 0−5 nm; (d) 0−20° z scale phase angle image corresponding to the area of (b).

the sudden change in height at this edge and is not indicative of a compositional change.

The mixed film prepared from combining the solutions of α- and ω-gliadin in the proportions 1:3 is shown in Figure 4a,b. Qualitatively it appears to be similar to the image shown in Figure 3a. However, close inspection reveals a small but marked phase angle difference of 2−3° between the raised portion of the topograph and the background. This observed difference may be compared with that of the mixed LB film shown in Figure 2b. If the adhesive interaction is greater for hydrophilic material than for hydrophobic, then a possible assignment of the raised region of Figure 4c as α-gliadin may be made. Utilizing a bearing analysis, the percentage of the surface area covered by the raised portion for the 400 μm^2 area of Figure 4a is 27 ± 1%, which is in good agreement with the proportion of α-gliadin in the deposited protein solution (25%).

Increasing the proportion of α-gliadin in the deposition solution also led to a subtle change in the surface morphology. Figure 5 shows the surface morphology obtained when a mixed solution of α- and ω-gliadin in equal proportions is evaporated. The images were obtained from several areas of the sample and show two types of surface coverage. In some areas, the coverage resembles that of the 1:3 α/ω adsorbed film, for example, Figure 5a, whereas in other regions a uniform surface coverage of spheroidal structures of average diameter ∼100 nm is observed (Figure 5c). In some parts (Figure 5d), the character of the surface coverage shows elements of both of these textures, with some circular and extended structures. The inset shows such structures at higher resolution. There is also evidence from phase angle measurement that these isolated higher structures give a higher phase shift than the background.

The origin of these surface patterns lies in the phase separation of the protein components as the volatile solution evaporates. A polymer science approach argued from a consideration of the free energies predicts two types of structure pattern on phase separation of a binary mixture. The two mechanisms are nucleation and growth and spinodal decomposition; the former results in a structure pattern of spherical precipitates, and the latter results in a pattern of interpenetrating phases (Strobl, 1997). It is apparent that both of these mechanisms are possible for the 1:1 α/ω mixed solution. Starting with a composition of 75% α-gliadin and 25% ω-gliadin, the resulting adsorbed film on mica shows the pattern associated with nucleation and growth (Figure 6). The spherical particulates are of a size similar to those seen in the equal proportion mixture.

A pure α-gliadin starting solution gives a characteristic morphology of surface coverage. At low and medium resolution (Figure 7a,b), a linked network of protein of height 2−2.5 nm is overlaid on the background. At high resolution (Figure 7c), it becomes clear that the whole surface consists of the same basic building block. The size of these structures, 5−10 nm, is consistent with the known dimensions of the α-gliadin molecule from STM and X-ray data, and resolution of the α-gliadin molecule has been achieved with this system (Shewry et al., 1997; Thomson et al., 1999). The phase angle data (Figure 7d)

corresponding to Figure 7b show no variation in intensity across the image area, other than that due to edge effects arising from sharp changes in topography at and near the edges of features, thus confirming the single protein composition of the deposited solution.

CONCLUSIONS

The morphology of gliadin films on mica has been successfully imaged using AFM. Monitoring the cantilever phase angle differences and the topography has permitted the differentiation of protein structural domains in both LB films and adsorbed films. For both types of deposited structures, the measurement of cantilever phase angle shows no variation in contrast and, hence, no variation in composition, for the single-protein samples. For the LB film of the mixed α- and ω-gliadins, the two protein components are observed to separate into large-scale phases extending over hundreds of square micrometers. For mixed films adsorbed from solution, the surface morphology is markedly different, and the phase angle variation is more subtle. The film produced from a 1:3 α/ω mixture shows a phase angle difference of several degrees between two components of the surface, and analysis of the surface coverage confirms that the higher phase angle component is present in the correct proportion for the starting composition. The phase angle results from the other mixtures are less clear, and this may reflect the more complex morphologies associated with these films. For the films produced from mixtures of α- and ω-gliadins, the surface textures show the two types of surface pattern expected from phase separation of a binary mixture. This suggests that the mechanism of spinodal decomposition is favored when the α-gliadin is the majority component and that nucleation and growth is favored when the ω-gliadin is dominant.

The separation into phases presumably results from differences in the structures and properties of the proteins, resulting in immiscibility. The ability of the ω-gliadin to form intra- and intermolecular hydrogen bonds and the relative occurrences of charged amino acid groups in the two proteins may be two important factors that affect miscibility. Similarly, the differences between the molecular conformations of the globular α-gliadin and the supposedly rodlike ω-gliadin may lead to differences in packing morphology.

The observation of protein microphases in the protein films may be relevant to the behavior of the proteins in the developing grain and in gluten and dough. The gluten proteins are deposited into discrete protein bodies in the developing endosperm cells, which ultimately fuse to form a continuous matrix. These protein bodies contain small inclusions of storage globulins, called triticins (Bechtel et al., 1991), which are presumably immiscible with the prolamins due to their fundamentally different conformations, compositions, and solubility properties. However, the major part of the protein body is homogeneous and has been assumed to consist of a random mixture of the different types of gluten proteins. Our results indicate that microphases could also be present in these protein bodies, although their similar staining properties mean they cannot be detected by conventional transmission electron microscopy.

On dough mixing the gluten matrix present in differing cells is brought together to form a continuous network. In addition, mixing is considered to optimize protein−protein interactions, leading to increased viscoelasticity, until overmixing leads to breakdown. It is possible, therefore, that the increased viscoelasticity during mixing results from, at least in part, the bringing together of microphases to form more extensive arrays of closely related proteins. The measurement of phase angle shifts of such systems, and other mixed biopolymer systems, has the potential to give much detailed information on the structure of such materials.

LITERATURE CITED

Bechtel, D. B.; Wilson, J. D.; Shewry, P. R. Immunocytochemical localisation of the wheat storage protein triticin in developing endosperm tissue. *Cereal Chem.* **1991**, *68*, 573−577.

Bergkvist, M.; Carlsson, J.; Karlsson, T.; Oscarsson, S. TM-AFM threshold analysis of macromolecular orientation: A study of the orientation of IgG and IgE on mica surfaces. *J. Colloid Interface Sci.* **1998**, *206*, 475−481.

Cole, E. W.; Kasarda, D. D.; Lafiandra, D. The conformational structure of A-gliadin. Intrinsic viscosities under conditions approaching the native state and under denaturing conditions. *Biochim. Biophys. Acta* **1984**, *787*, 244−251.

Field, J. M.; Tatham, A. S.; Baker, A. M.; Shewry, P. R. The structure of C hordein. *FEBS Lett.* **1986**, *200*, 76−80.

Furuno, T.; Sasabe, H.; Ikegami, A. Imaging two-dimensional arrays of soluble proteins by atomic force microscopy in contact mode using sharp supertip. *Ultramicroscopy* **1998**, *70*, 125−131.

Garcia, R.; Tamayo, J.; Calleja, M.; Garcia, F. Phase contrast in tapping-mode scanning force microscopy. *Appl. Phys. A: Mater. Sci. Process.* **1998**, *66*, S309−S312.

Hallet, P. C.; Tskhovrebova, L.; Trinick, J.; Offer, G.; Miles, M. J. Improvements in atomic force microscopy protocols for imaging fibrous proteins. *J. Vac. Sci. Technol. B* **1996**, *14*, 1444−1448.

Leggett, G. J.; Davies, M. C.; Jackson, D. E.; Tendler, S. J. B. Scanning probe microscopy of biomolecules and polymeric biomaterials. *J. Electron Spectrosc. Relat. Phenom.* **1996**, *81*, 249−268.

Marchant, R. E.; Barb, M. D.; Shainoff, J. R.; Eppell, S. J.; Wilson, D. L.; Siedlecki, C. A. Three-dimensional structure of human fibrinogen under aqueous conditions visualized by atomic force microscopy. *Thromb. Haemostasis* **1997**, *77*, 1048−1051.

McMaster, T. J.; Miles, M. J.; Walsby, A. E. Direct observation of protein secondary structure in gas vesicles by atomic force microscopy. *Biophys. J.* **1996**, *70*, 2432−2436.

Müller, D. G.; Schoenenberger, C. A.; Schabert, F.; Engel, A. Structural changes in native membrane proteins monitored at subnanometer resolution with the atomic force microscope: A review. *Struct. Biol.* **1997**, *119*, 149−157.

Müller, D. J.; Fotiadas, D.; Engel, A. Mapping flexible protein domains at subnanometer resolution with the atomic force microscope. *FEBS Lett.* **1998**, *430*, 105−111.

Ohnishi, S.; Hara, M.; Furuno, T.; Sasabe, H. Imaging two-dimensional crystals of catalase by atomic force microscopy. *Jpn. J. Appl. Phys.* **1996**, *35*, 6233−6238.

Rakowska, A.; Danker, T.; Schneider, S. W.; Oberleithner, H. ATP-induced shape change of nuclear pores visualised with the atomic force microscope. *J. Membr. Biol.* **1998**, *163*, 129−136.

Schneider, S. W.; Larmer, J.; Henderson, R. M.; Oberleithner, H. Molecular weights of individual proteins correlate with molecular volumes measured by atomic force microscope. *Pfluegers Arch. Eur. J. Physiol.* **1998**, *435*, 362−367.

Shewry, P. R.; Tatham, A. S. The prolamin storage proteins of cereal seeds: structure and evolution. *Biochem. J.* **1990**, *267*, 1−12.

Shewry, P. R.; Tatham, A. S. Disulphide bonds in wheat gluten proteins. *J. Cereal Sci.* **1997**, *25*, 207−227.

Shewry, P. R.; Miles, M. J.; Thomson, N. H.; Tatham, A. S. Scanning probe microscopies—applications in cereal science. *Cereal Chem*. **1997**, *74* (4), 193−199.

Strobl, G. R. *The Physics of Polymers*, 2nd ed.; Springer-Verlag: Berlin, Germany, 1997.

Tatham, A. S.; Shewry, P. R. The conformations of wheat gluten proteins. The secondary structures and thermal stabilities of the α-, *β*-, *γ*- and *ω*-gliadins. *J. Cereal Sci.* **1985**, *3*, 103−113.

Tatham, A. S.; Shewry, P. R. The S-poor prolamins of wheat, barley and rye. *J. Cereal Sci.* **1995**, *22*, 1−16.

Tatham, A. S.; Drake, A. F.; Shewry, P. R. Conformational studies of a synthetic peptide corresponding to the repeat motif of C hordein. *Biochem. J.* **1989**, *259*, 471−476.

Thomson, N. H.; Miles, M. J.; Popineau, Y.; Harries, J.; Shewry, P.; Tatham, A. S. Small-angle X-ray scattering of wheat seed-storage proteins: α-, *γ*- and *ω*-gliadins and the high molecular weight (HMW) subunits of glutenin. *Biochim. Biophys. Acta Protein Struct. Mol. Enzymol.* **1999**, *1430*, 359−366.

van Noort, S. J. T.; van der Werf, K. O.; Eker, A. P. M.; Wyman, C.; de Grooth, B. G.; van Hulst, N. F.; Greve, J. Direct visualisation of dynamic protein-DNA interactions with a dedicated atomic force microscope. *Biophys. J.* **1998**, *74*, 2840−2849.

Wannerberger, L.; Nylander, T.; Eliasson, A. C.; Tatham, A. S.; Fido, R. J.; Miles, M. J.; McMaster, T. J. Interaction between α-gliadin layers. *J. Cereal Sci.* **1997**, *26*, 1−13.

Wellner, N.; Belton, P. S.; Tatham, A. S. Fourier transform IR spectroscopy of hydration-induced structure changes in the solid state of omega-gliadins. *Biochem. J.* **1996**, *319*, 741−747.

Woychik, J. H.; Boundy, J. A.; Dimler, R. J. Starch gel electrophoresis of wheat gluten proteins with concentrated urea. *Arch. Biochem. Biophys.* **1961**, *94*, 477−482.

Received for review March 24, 1999. Revised manuscript received August 25, 1999. Accepted September 15, 1999. IACR receives grant-aided support from the Biotechnology and Biological Sciences Research Council of the United Kingdom.

JF9904057